An integrative bioinformatics approach to decipher adipocyte-induced transdifferentiation of osteoblast

Ayyoub Salmi, Federica Quacquarelli, Christophe Chauveau, Aline Clabaut, Odile Broux

Genomics 114 (2022) 110422

Contents lists available at ScienceDirect

Genomics

journal homepage: www.elsevier.com/locate/ygeno

An integrative bioinformatics approach to decipher adipocyte-induced transdifferentiation of osteoblast

Ayyoub Salmi [1], Federica Quacquarelli [1], Christophe Chauveau, Aline Clabaut, Odile Broux [*]

Univ. Littoral Côte d'Opale F-62200 Boulogne-sur-Mer, France, Univ. Lille F-59000, Marrow Adiposity and Bone Lab – MABLab, ULR 4490 Lille, France

ARTICLE INFO

Keywords:
Human bone marrow stromal cells
Osteoblast
Adipocyte
Transdifferentiation
Multi-omics
Cellular crosstalk

ABSTRACT

In human, bone loss is associated with increased marrow adipose tissue and recent data suggest that medullary adipocytes could play a role in osteoporosis by acting on neighboring bone-forming osteoblasts. Supporting this hypothesis, we previously showed, in a coculture model based on human bone marrow stromal cells, that factors secreted by adipocytes induced the conversion of osteoblasts towards an adipocyte-like phenotype. In this work, we employed an original integrative bioinformatics approach connecting proteomic and transcriptomic data from adipocytes and osteoblasts, respectively, to investigate the mechanisms underlying their crosstalk. Our analysis identified a total of 271 predicted physical interactions between adipocyte-secreted proteins and osteoblast membrane protein coding genes and proposed three pathways for their potential contribution to osteoblast transdifferentiation, the PI3K-AKT, the JAK2-STAT3 and the SMAD pathways. Our findings demonstrated the effectiveness of our integrative omics strategy to decipher cell-cell communication events.

1. Introduction

Maintenance of healthy bone mass requires a continuous process of bone remodelling, which consists of a balance of bone resorption by osteoclasts and bone formation by osteoblasts. With advancing age, an impairment of this balance results in osteoporosis due to a reduction in bone mass associated with a high risk of fragility fractures. It is most often due to an excess in osteoclastic activity that is not sufficiently compensated by bone formation [1]. A strong relationship between this bone loss and an increase in bone marrow adipose tissue suggests a potential role for medullary adipocytes in the deficiency of osteoblasts to replace the resorpted bone [2–4]. This hypothesis is supported by the proximity of adipocytes to osteoblasts, their shared mesenchymal origin and the fact that adipocytes are secretory cells [5]. In an attempt to reproduce cellular interactions within the bone marrow, we previously developed a coculture system using human bone marrow stromal cells (BMSCs) – derived osteoblasts and adipocytes. In this model, we demonstrated that soluble factors secreted by adipocytes induced the conversion of osteoblasts towards an adipocyte-like phenotype, as evidenced by the expression of adipogenic mRNA markers and a decrease in levels of osteogenic mRNA markers [6]. This change in fate was further confirmed by microarray gene expression profiling showing profound transcriptomic changes in osteoblasts with an enrichment in the adipocyte gene signature following coculture. Furthermore, double immunofluorescence staining demonstrated the co-expression of adipogenic and osteogenic specific markers at the single cell level providing evidence for a transdifferentiation event [7]. To characterize the adipocyte-secreted factor(s) implicated in the transdifferentiation of osteoblasts, we thus used high-throughput proteomic techniques to identify a set of secreted proteins potentially regulators of osteoblast differentiation [8]. Subsequently, through transcriptomic analysis of the osteoblastic population, gene expression changes induced by adipocyte secretion products in the osteoblastic cells were identified at two early stages of coculture. The results showed that the phenotype conversion was initiated as early as 9 h of coculture and then progressed in a dynamic process. Specifically, Gene Ontology analysis of differentially expressed genes in osteoblasts upon 9 h of coculture revealed increased expression of genes associated with regulation of cellular communication and cell signaling, while most of the adipogenesis-related transcripts were gradually up-regulated from 9 to 48 h [7].

In the present work, we developed an original integrative bioinformatics approach connecting proteomic and transcriptomic data from both cell types to decipher the molecular mechanisms underlying the crosstalk between adipocytes and osteoblasts. The combined use of

* Corresponding author.
E-mail address: broux@univ-littoral.fr (O. Broux).
[1] Co- first authors

https://doi.org/10.1016/j.ygeno.2022.110422
Received 18 February 2022; Received in revised form 9 June 2022; Accepted 28 June 2022
Available online 9 July 2022

protein-protein interaction networks and gene set enrichment analyses allowed us to integrate paired ligand-receptor and downstream signaling elements to propose significant pathways that may promote osteoblast transdifferentiation.

2. Methods

2.1. Cell culture experiments

2.1.1. Cell culture and induction of osteogenic and adipogenic differentiation

Human BMSCs (Lonza, Belgium; Rosterbio, USA) at passage 4 to 6 were plated in 6-well plates in expansion medium composed of Dulbecco's Modified Eagle Medium (DMEM) (Pan Biotech, Dutscher, France) containing 10% fetal calf serum (FCS, Pan Biotech, Dutscher), 1% penicillin/streptomycin and 1% glutamine (Dutscher). Cell cultures were maintained at 37 °C in a humidified atmosphere of 95% air and 5% CO2, and the media were changed twice weekly. Differentiation experiments were started when BMSCs had reached confluence (D0). To induce osteogenesis, BMSCs were cultured in DMEM with 10% FCS supplemented with osteogenic inducers (50 μM ascorbic acid, 10 mM β-glycerophosphate and 10–8 M vitamin D3 (Sigma-Aldrich, France)) for 14 days. For adipogenic differentiation, BMSCs were cultured in DMEM with 10% FCS supplemented with adipogenic inducers (0.5 μM dexamethasone, 0.5 mM isobutyl-1-methylxanthine and 50 μM indomethacin (Sigma-Aldrich)) for 10 or 14 days.

2.1.2. Conditioned medium experiments

Two different methods were used to prepare the adipocyte conditioned media, Serum Free culture in Adipogenic medium (SFA) and PBS Washing (W). In the first one, at day 10 of differentiation, BMSC-derived adipocytes were incubated in serum-free DMEM supplemented with adipogenic inducers. At day 14, the cells were placed in serum-free DMEM and supernatants were collected at day 16. In the washing strategy, at day 14 of differentiation, BMSC-derived adipocytes were washed twice with 4 ml of PBS (Dutscher) before serum-free DMEM was added. Supernatants were collected at day 16. For each method, the supernatants were then applied to BMSC-derived osteoblasts at day 14 of differentiation. Osteoblasts were incubated in conditioned medium for 48 h (OB-CM). As controls, osteoblasts were incubated with serum-free DMEM for the same time (OB).

2.2. RNA expression measurement

2.2.1. RNA isolation

Total RNA was extracted using the RNeasy® Micro Kit, including the DNase I digestion step (Qiagen, France), according to the manufacturer's instructions and quantified by Nanodrop at the wavelength of 260 nm.

2.2.2. mRNA expression analysis

Total RNA was reverse transcribed using Maxima First-Strand cDNA Synthesis kit (Fermentas, Thermoscientific, France), and subjected to quantitative real-time PCR on the LightCycler® Carousel-Based System (Roche Diagnostics, France) using the LightCycler® Fast Start DNA Master SYBR® Green I kit and specific primers designed using Oligo 6 software (MedProbe, Norway). Protocol consisted of a hot start step (8 min at 95 °C) followed by 40 cycles including a 10 s denaturation step at 95 °C, a 10 s annealing step, and an elongation step at 72 °C varying from 3 s to 11 s. The primer sequences and PCR conditions are given in Table 1. Relative gene expression levels were normalized to YWHAZ (tyrosine 3-monooxygenase/tryptophan 5-monooxygenase activation protein), and PPIA (peptidylprolyl isomerase A) transcripts and determined using the 2−ΔΔCt method. Quantification data represented the mean ± standard deviation (SD) of at least four experiments performed in duplicate. For the statistical analysis, differences between the OB and OB-CM groups were compared using the Mann-Whitney test. A p-value of <0.05 was set as statistically significant.

2.3. Bioinformatic analysis

2.3.1. Adipocyte secretome data analysis

Secreted proteins present in the adipocyte culture supernatants prepared with SFA or W methods were analyzed in a previous work on three biological experiments by LC-MS/MS and label-free quantification [8]. Expression levels of secreted proteins from depleted and rinsed media were first compared to retain only proteins expressed in depleted medium with a fold change >1.3 across at least two samples in LC MS/MS data. In label-free data, the mean expression for depleted and rinsed samples were used. Actively secreted proteins were selected based on their association with the "extracellular matrix" (GO:0031012) or "extracellular space" (GO:0005615) gene ontology (GO) terms from NCBI and Ensembl GO annotations.

2.3.2. Membranome data analysis

Transcriptional changes were previously monitored in 7 biological replicates, each consisting of osteoblasts grown alone and cocultured osteoblasts after 9 h or 48 h, using the Agilent Human SurePrint G3 Microarray, 8 × 60 K microarray chip (Agilent Technologies) [7].

Microarray data have been deposited in the Array Express data base at EMBL-EBI (https://www.ebi.ac.uk/arrayexpress/experiments/E-MTAB-8849/). Probe-level data were preprocessed using LIMMA [9] by applying the normexp background correction method followed by within-array normalization using the robust spline method, and between-array normalization using the Aquantile method. The totality of the genes expressed in osteoblasts were selected for membranome identification from transcriptomic data using a background expression cutoff corresponding to two times the overall median log2-transformed probe intensity. For the definition of membrane protein-coding genes, we made use of the *in silico* human surfaceome [10] that consists of a list of cell-surface proteins predicted using machine learning. The membranome was then defined as the intersection of the total genes expressed in osteoblasts and the genes from the *in silico* human surfaceome.

Table 1
Primer sequences and conditions of PCR.

cDNA	GenBank	Forward and reverse primers	Product (bp)	Ta (°C)	Elongation (s)
CEBPA	NM_004364	F: 5′ - ACTGGGACCCTCAGCCTTG −3′ R: 5′ - TGGACTGATCGTGCTTCGTG - 3’	75	55	3
PPARG	NM_015869	F: 5’-GCTTCTGGATTTCACTATGG −3′ R: 5′- AAACCTGATGGCATTATGAG −3’	195	54	8
PPIA	NM_021130	F: 5’- ACCGTGTTCTTCGACATTGC -3′ R: 5′- CAGGACCCGTATGCTTTAGGA −3’	274	60	11
YWHAZ	NM_145690	F: 5’- GGTCATCTTGGAGGGTCGTC -3′ R: 5′- GTCATCACCAGCGGCAAC -3’	245	56	10

Shown are GenBank accession numbers, primer sequences, lengths of the PCR products in base pairs, annealing temperatures (Ta), and elongation times in seconds. F: Forward; R: Reverse. CEBPA, CCAAT/enhancer-binding protein alpha; PPARG: Peroxisome proliferator-activated receptor gamma; PPIA: peptidylpropyl isomerase A; YWHAZ: Tyrosine 3-monooxygenase/tryptophan 5-monooxygenase activation protein.

2.3.3. Protein-protein interactions

Protein-protein interactions between secreted proteins and cell-surface proteins were obtained from StringDB [11]. A minimum interaction score of 0.9, corresponding to the probability that a link exists between two proteins, was used to select only the highest confidence interactions.

2.3.4. Gene set enrichment analysis

Downstream effects of the interactions between secreted proteins and cell-surface proteins were investigated by looking for relevant pathways. Differentially expressed genes in co-cultured osteoblasts at 9 h and 48 h were used for gene set enrichment analysis (GSEA). Enrichment scores were calculated as follow, based on the GSEA method [12]:

1. Genes were assigned a rank metric S(G*i*) using the following formula, then they were sorted in decreasing order

$$S(G_i) = -sign(FC_i).log_2(|FC_i|).log_{10}(pvalue_i)$$

2. Pathway genes from WikiPathways were used as gene sets for this analysis [13]. Two running statistics corresponding to the fraction of genes in the set (hits) and genes that are not in the set (misses) were calculated up to a given position *i*, defined as

$$P_{hit}(S,i) = \sum_{\substack{g_j \in S \\ j \le i}} \frac{|r_j|^p}{N_r}$$

$$P_{miss}(S,i) = \sum_{\substack{g_j \notin S \\ j \le i}} \frac{1}{N - N_H}$$

where $N_r = \sum_{g_i \in S} |s_i|^{p\cdot}$, N is the number of input genes, NH is the number of genes in the set, rj is the correlation score, and P is the step weight.

3. Enrichment score for pathways were calculated using a weighted Kolmogorov Smirnov (K—S) statistic defined as follow

$$ES = \sup_x |P_{hit}(x) - P_{miss}(x)|$$

4. The null distribution was derived by using a resampling method that involves randomly permuting the ranked gene list and recalculating the corresponding enrichment score $S^{GSEA}_{K,\pi p}$ for Nk = 1000 times, the p-value is then defined as the fraction of enrichment scores greater than the initially observed enrichment score

$$Pval = \frac{1}{N_K} \sum_{p=1}^{N_K} I\left\{S^{GSEA}_{K,\pi p} \ge S^{GSEA}_K\right\}$$

5. Finally, a multiple testing correction was applied using the false discovery rate (FDR) method and the enrichment scores were normalized to account for gene set size using the formula

$$\frac{S^{GSEA}_K}{E\left[S^{GSEA}_{K,\pi p}\right]}$$

3. Results

3.1. Experimental study design and workflow

To identify adipocyte-secreted factor(s) causing a shift of osteoblasts towards an adipocyte-like phenotype, we used an integrative Omics strategy combining proteomic and transcriptomic data from both cell types as shown in Fig. 1. We first identified proteins contained in adipocyte culture media using LC MS/MS and Label Free methods and selected actively secreted proteins using Gene Ontology terms. In parallel, by combining gene expression data experimentally determined in osteoblasts and data from the *in silico* human surfaceome, we identified protein coding genes that are part of the osteoblast membranome. Physical interactions between adipocyte secreted proteins and osteoblast membrane proteins were then investigated using data from StringDB. Finally, significant pathways leading to osteoblast transcriptional changes were identified using gene set enrichment analysis (GSEA). The bioinformatics method developed in this work is available as a stand-alone java application at https://bio.tools/intomics.

3.2. Generation of stimulatory and non-stimulatory adipocyte conditioned media

One crucial point in analyzing cellular secretome collected as conditioned medium is cross contamination by cell culture media components, especially bovine serum proteins. In view of serum removal in conditioned media, two methods were previously investigated, PBS Washing (W) and Serum Free culture in Adipogenic medium (SFA) [8]. Cells were either washed twice with PBS (W method) or cultured the last four days of differentiation in serum free adipogenic medium (SFA method). In both cases, they were subsequently incubated in serum free medium during 48 h before collection of the supernatants. The efficiency of serum removal in conditioned media was confirmed by acrylamide gel electrophoresis, clearly showing the removal of the albumin band for both preparation methods. However, real-time PCR experiments revealed that PBS washes induced severe modifications of the phenotype of rinsed cells, with a loss of specific features of adipocytes compared with adipocyte control or cells cultured in SFA medium [8]. Although these changes in cellular phenotype can be expected to cause modifications in the secretome as well, we were very surprised to observe that the conditioned medium of the rinsed adipocytes had no more effect on the osteoblasts. As shown in Fig. 2, the consistent increase in the mRNA levels of adipogenic markers, such as PPARG (Peroxisome Proliferator Activated Receptor Gamma) and CEBPA (CCAAT Enhancer Binding Protein Alpha) previously reported in osteoblasts following incubation with adipocyte conditioned medium, was observed for osteoblasts incubated with adipocyte supernatant obtained with the SFA method but not with the W method. We thus decided to compare the non stimulatory medium obtained with the W method *versus* medium obtained using SFA method to find adipocyte-secreted factors implicated in the conversion of osteoblasts.

3.3. Differential adipocyte secretome analysis

One dimensional LC-MS/MS and label-free quantification were used to compare secreted proteins present in the culture supernatants prepared by SFA and W methods. If many of the proteins were identified in conditioned media prepared with the two methods, quite a few proteins were however selectively identified in W and SFA preparations, respectively [8]. Among the 2037 identified proteins using LC MS/MS, 477 were identified as actively secreted by adipocytes based on GO information, while 81 proteins displayed a significantly higher expression

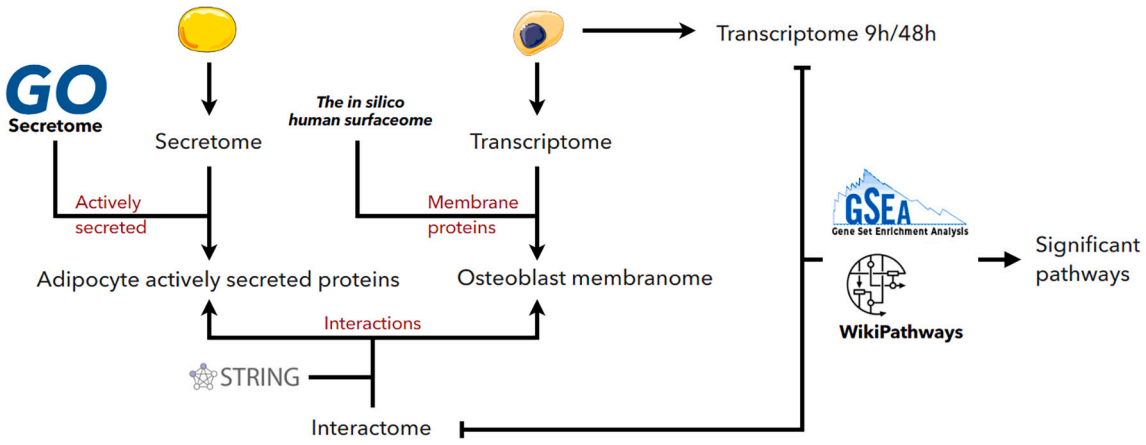

Fig. 1. Schematic overview of experimental workflow for the determination of pathways involved in osteoblast transdifferentiation, using data from the adipocyte secretome and the osteoblast transcriptome. GO: Gene Ontology; GSEA: Gene set enrichment analysis.

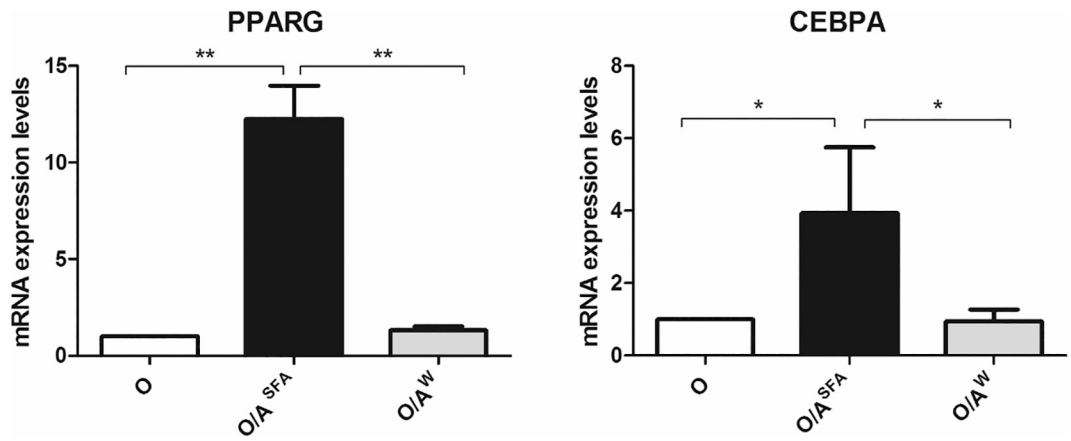

Fig. 2. Quantitative RT-PCR analysis of adipocyte-specific genes, PPARG (Peroxisome Proliferator Activated Receptor Gamma) and CEBPA (CCAAT Enhancer Binding Protein Alpha). O: Osteoblast in serum free medium for 48 h. O/A^{SFA}: Osteoblasts incubated for 48 h with adipocyte supernatant obtained with the SFA (Serum Free Adipogenic medium) method. O/A^{W}: Osteoblasts incubated for 48 h with adipocyte supernatant obtained with the W (PBS washing) method. mRNA expression levels were normalized against the signal from two housekeeping genes for peptidylprolyl isomerase A (PPIA) and tyrosine 3-monooxygenase/tryptophan 5-monooxygenase activation protein (YWHAZ).
Bars represent the mean ± standard error of at least four independent experiments. * $p < 0.05$, ** $p < 0.005$.

level in SFA samples. As for label free data, 88 proteins out of 1691 were identified as actively secreted, of which 22 showed a significantly higher expression level in depleted samples (Fig. 3). The list of proteins over-expressed in SFA samples are shown in Supplementary Table S1.

3.4. Osteoblast membranome identification

Gene expression analyses of the osteoblastic population were previously performed by microarray in 7 biological replicates [7]. Using those available data, we applied a cutoff corresponding to two times the overall median log2-transformed probe intensity (*i.e.* 8.72) and thus selected 2885 genes expressed in osteoblasts. Gene-encoding membrane proteins were then selected based on their association with the *in silico* human surfaceome database. We found that 454 protein coding genes expressed in osteoblasts were associated with gene products located on the surface membrane (Supplementary Table S2).

3.5. Prediction of interaction networks

In order to examine the effects of adipocyte secreted proteins on osteoblast surface membrane proteins, we combined osteoblast membranome data and adipocyte secretome data with protein-protein interaction information. The network of interactions consisted of 22 adipocyte-secreted proteins interacting with 55 osteoblast membranome protein coding genes, for a total of 62 predicted physical interactions using label free data, and 81 adipocyte-secreted proteins interacting with 71 osteoblast membranome protein coding genes, for a total of 223 predicted physical interactions using LC MS/MS data (Fig. 4). A graphical representation edited for clarity, showing this complex network of interactions between secreted proteins and membrane proteins, revealed some well-known connections such as the association of LEP (leptin), one of the major proteins secreted by adipocytes, with LEPR (leptin receptor), and ANGPT4 (Angiopoietin4) with TEK (TEK Receptor Tyrosine Kinase) (Fig. 5).

3.6. Candidate pathways leading to transdifferentiation

Data for differentially expressed genes in cocultured osteoblasts at 9 and 48 h compared to osteoblasts grown alone were used for gene set enrichment analysis to further determine the process behind the transdifferentiation of osteoblasts towards an adipocyte-like phenotype (Table S3). It allowed us to find pathways significantly affected by the coculture (Table 2). Among them, we focused particularly on three pathways known for their involvement in the regulation of osteogenesis

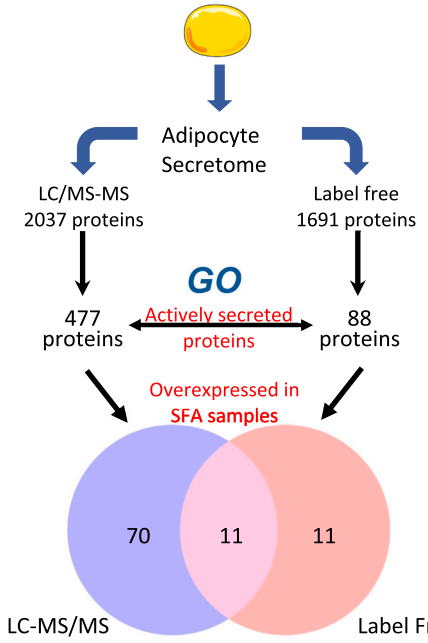

Fig. 3. Schematic representation of the method used to determine the differential adipocyte secretome by LC/MS-MS and Label Free. GO: Gene Ontology; SFA: Serum Free culture in Adipogenic medium.

and adipogenesis (Fig. 6). Two of these pathways could be activated, the PI3K-AKT (phosphatidylinositol 3-kinase- protein kinase B) pathway and the JAK2-STAT3 (Janus kinase 2/signal transducers and activators of transcription 3) pathway, following the binding of IGF2 (Insulin-like Growth Factor 2), ANGPT4 or LEP to their respective receptor. Supporting this assumption, we observed an increase in the expression of related effectors, such as IRS2 (Insulin Receptor Substrate 2) and PI3K along with downstream key adipogenic markers, KLF5 (Kruppel Like Factor 5), CEBPA and PPARG (Fig. 5). On the other side, our analyses indicated that signaling by TGF-beta (transforming growth factor-beta) superfamily members seemed to be down-regulated. This inhibition could be mediated by competitive binding of INHBB (Inhibin Subunit Beta B) to ACVR2A (Activin A Receptor Type 2A), with additional help of soluble TGFBR3 (Transforming Growth Factor-Beta Receptor Type III) which acts as a co-receptor to strengthen its inhibition. Another negative regulator, Noggin, present in adipocyte secretome, could participate to this downregulation by antagonizing BMP (Bone Morphogenic Protein) signaling. In our hypothesis, the intracellular signals transduced mainly through SMAD would further repress the transcription of specific target genes involved in osteoblastic differentiation, such as RUNX2 (RUNX Family Transcription Factor 2).

4. Discussion

Bone marrow stromal cells are able to differentiate into the cell lineages responsible for bone and fat formation, osteoblasts and adipocytes [14–17]. In humans, it has been demonstrated that osteoporosis bone loss is accompanied by an increase in the number of medullary adipocytes [3,4,18,and]. It has been suggested that this extension of marrow adipose tissue is mainly due to a preferential differentiation of the bone marrow stromal precursors towards the adipogenic lineage [19,20]. It is also conceivable that the increased adipose tissue may have a negative impact on neighboring osteoblast by a paracrine effect [21]. Supporting this hypothesis, we previously showed in a coculture model that soluble factors secreted by adipocytes induced the conversion of osteoblasts towards an adipocyte-like phenotype [6]. This finding was further supported by double immunofluorescence staining that provided evidence for a hybrid phenotype in cocultured osteoblasts indicative of a partial transdifferentiation event [7]. Our aim was to decipher the paracrine factors and the downstream signaling within the osteoblasts that promoted this change in fate. For this, on one side, we analyzed and compared stimulatory and non-stimulatory adipocyte culture supernatants to select a pool of candidate secreted factors. On the other side, we determined transcriptional changes induced by a 9 or 48 h coculture in osteoblasts. To connect these omics data, computational approaches are critical. In the past several years, there were great advances in informatics tools for processing large molecular data sets [22]. Algorithms have been developed for integrating transcriptomic and proteomic dimensions from the same cell but to our knowledge they are not suited for deciphering intercellular crosstalk, due to the fact that they rely on data from either the same or overlapping set of samples. To solve this issue, our strategy was (1) to couple a ligand to its receptor and to examine the genes and signaling pathways potentially regulated by the activation of this receptor and (2) to use computational methods to confront the components of these signaling pathways with the observed transcriptomic changes. For the first step, we took our cue from an approach described in other models [23,24] to investigate protein-protein interactions between members of the adipocyte secretome and members of the osteoblast membranome. Then data from differentially expressed genes in cocultured osteoblasts were used for GSEA with a method slightly different than the ones proposed by Subramanian et al. [12]. The combined use of protein-protein interaction and gene set analyses to integrate our experimental biological data allowed us to take full advantage of both pathway structure and activity. In addition, the

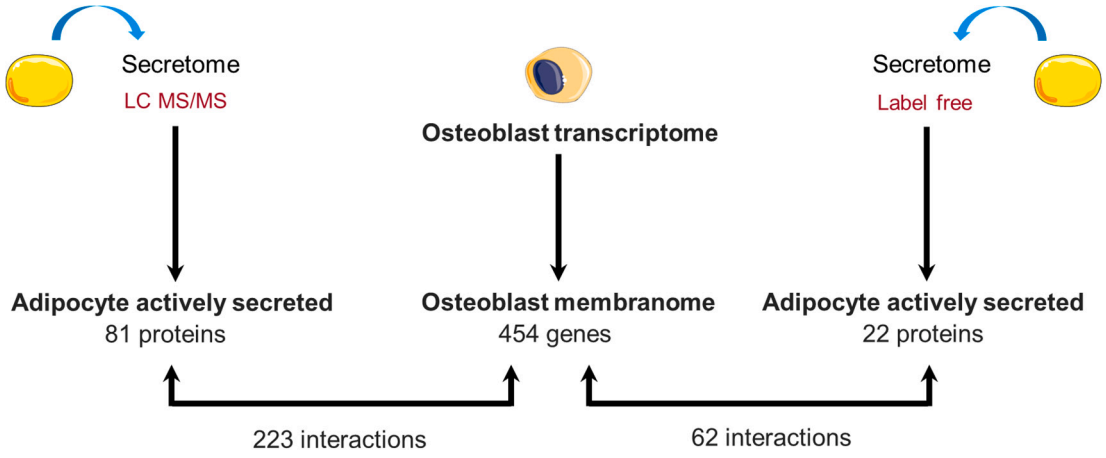

Fig. 4. Prediction of interaction networks. Diagram showing the number of protein-protein interactions between actively adipocyte-secreted proteins identified using LC MS/MS and label free, respectively and osteoblast gene-encoding membrane proteins.

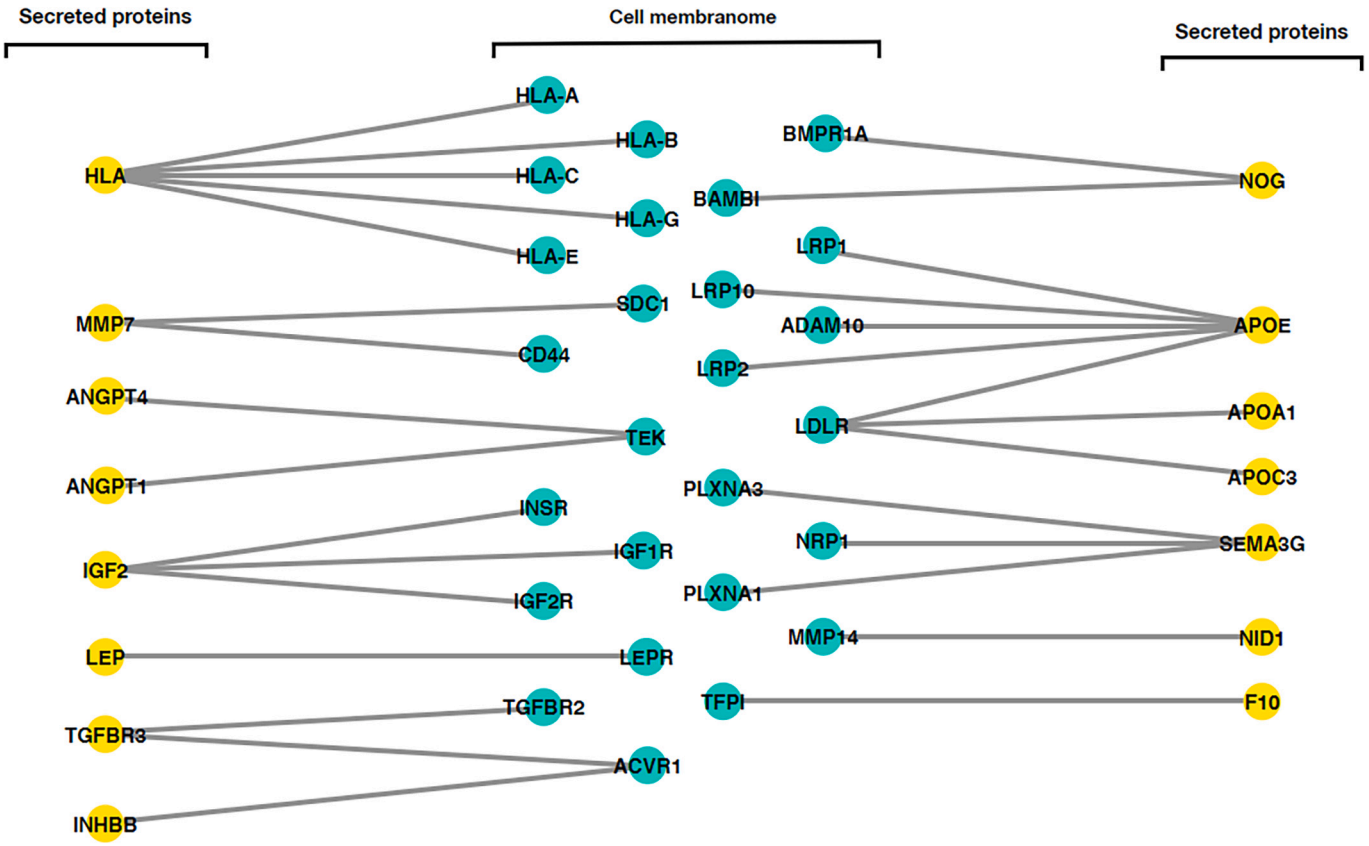

Fig. 5. Graphical representation showing examples of interactions between adipocyte secreted proteins (in yellow) and osteoblast proteins from cell membranome (in green). (For interpretation of the references to colour in this figure legend, the reader is referred to the web version of this article.)

availability of temporal gene expression data at two time points, 9 and 48 h, provided a more accurate understanding of the dynamic progression of the signal transduction process and led us to identify significant pathways that may promote osteoblast transdifferentiation.

PI3K is an important lipid kinase that controls a number of cellular functions in response to ligand activation and downstream activation of AKT. The upstream stimulators of the pathway include various biological molecules such as Epidermal Growth Factor (EGF), Insulin-Like Growth Factor (IGF), Insulin, and Platelet-Derived Growth Factor (PDGF). Among its well-known roles in regulating cellular proliferation, survival and migration, the PI3K-AKT pathway has also been shown to be important in the lineage commitment of BMSCs in spite of contradictory data regarding its role in adipogenesis and osteogenesis [25,26]. Indeed, it has been demonstrated that AKT promotes adipogenesis by increasing the expression of PPARG and CEBPA *via* the activation of Mammalian Target of Rapamycin (mTOR) [27]. On the other hand, in osteoblasts, AKT can also inactivate Forkhead transcription factors 1 and 3 (FOXO1,3) which leads to regulation of osteogenic genes such as RUNX2 and Osteocalcin [25]. Moreover, the abundant growth factors in bone matrix IGF-1 and IGF-2, signaling *via* the PI3K-AKT pathway, have both pro-osteogenic and pro-adipogenic properties [28]. The overlap of the PI3K-AKT pathway with other signaling networks lead to a great level of complexity that can explain its pleiotropic effect. In our hypothesis, this pathway could be activated and promote adipogenesis following the binding of IGF2 to IGF1R (Insulin-Like Growth Factor 1 Receptor) or/and INSR (Insulin Receptor) or ANGPT4 to the TEK receptor tyrosine kinase. The binding of leptin to its receptor LEPR activates various pathways including IRS/PI3K and JAK2/STAT3 with a subsequent role in the regulation of differentiation of BMSCs. Leptin has mainly been observed to promote osteogenesis and to inhibit adipogenesis by cultured stromal cells [29,30]. Conversely, other findings reported that LepR signaling in BMSCs promotes adipogenesis, reduces osteogenesis and impairs fracture healing [31,32]. These findings support the complexity of leptin signaling and it has been suggested that the differentiation stages of BMSCs as well as variables such as leptin concentration or serum condition can play a role in the effects of leptin *in vitro* [33].

According to our analysis, the transdifferentiation of osteoblasts could also be due to a down-regulation of the SMAD pathway leading to an inhibition of the expression of osteoblast genes such as RUNX2. SMAD mediates the signal from a great variety of different TGF-beta/BMP superfamily ligands such as TGFB, Activin or BMP [34,35]. The presence in the adipocyte secretome of INHBB and the proteoglycan TGFBR3, also known as Betaglycan, could antagonize Activin signaling by forming a stable complex and sequestering type II Activin Receptor and blocking downstream SMAD signaling. The adipocyte-secreted Noggin could also participate to this down-regulation by binding members of the BMP family in the extracellular space, preventing their interaction with both Type I and type II BMP receptors and inactivating downstream SMAD signaling. In our model, this anti-osteogenic effect was plausible in view of the decrease in expression level of a specific osteogenic marker, Osteocalcin, previously observed following coculture [6]. In consistence with our finding, an inhibitory effect of marrow adipocytes on osteogenesis mediated by BMP2 inactivation has previously been reported in mouse BMSCs [36].

Overall, the transcriptional changes observed in cocultured osteoblasts support the possible involvement of each of these pathways with both up-regulation of adipogenesis and down-regulation of osteogenesis, leading to the transdifferentiation process. However, in the course of our experimental efforts to decipher the mechanisms of this phenomenon, it has becoming increasingly clear that a single pathway cannot explain this change in fate and that multiple pathways, mediated by several secreted factors, act in concert. The nature of these major pathways involved in many cellular processes and their overlap lead to a

Table 2
Significant pathways identified by gene set enrichment analysis.

Pathway	p-value	Genes
Apoptosis	0.018	CDKN1A, HSPB1, IER3, F2R, NRG1, TNFRSF21, PTK2B, NET1, GCLC, BCL3
Binding and Uptake of Ligands by Scavenger Receptors	0.011	APOL1, SAA1
Cell surface interactions at the vascular wall	0.001	PIK3R1, SLC7A8, PF4, CAV1, TNFRSF10A, ITGAM, ITGA5, ANGPT2, ANGPT1, TEK
Cells and Molecules involved in local acute inflammatory response	0.008	VCAM1, C5, IL6
Class A/1 (Rhodopsin-like receptors)	0.001	AGTR1, FPR1, LPAR1, GNRH1, EDN1, PTGER1, PTGER2, XK, SAA1, PF4, GPR68, NPY2R, CCRL1, ADORA1, F2R, HRH1, DRD5, OPN3, HTR1F, CXCL12, GPER, CXCL1, ADRA1B, CXCL2, BDKRB2, BDKRB1, PTGIR, SSTR2, P2RY6, P2RY2, S1PR1, S1PR3
Clathrin-mediated endocytosis	0.013	FNBP1L, AGTR1, AMPH, SYNJ2, DAB2, HIP1, STON1, DNM3, DNAJC6, REPS2, EGF, HIP1R
Copper homeostasis	0.0	MT1L, MT1X, MT2A, CCND1, MT1A, MT1H, MT1B, STEAP2, TP53, MT1E, FOXO3, FOXO1, COX11, JUN
Degradation of the extracellular matrix	0.012	ADAMTS5, CDH1, MMP7, DCN, MMP11, MMP15, MMP19, LAMA3, LAMB1
Endoderm Differentiation	0.038	SESN1, MAP2K3, DKK1, NOTCH1, TCF7, GATA6, FOXO1, EPB41L5, SMAD3, FOXN3, TRERF1, EXT1, DAB2, RARG, SCHIP1, DUSP5, TET1, PARP8, PTHLH, TCEAL2
Endothelin Pathway	0.005	GLS, RPS6KA2, TNS1, EPHA2, WWTR1, JUN, RDX, SNAI1, ZNF131, TIMP3, IL11, EDN1, FOS, VEGFA, FGF2, RGS3, CCND1, CDH1, LEPR, FOXO3, VCAM1, NFKBIA, IL6, HSPB1, CXCL1, ITGA5, PTK2B, STOM, CCL2, PPP1R14A, MARCKS, COL7A1
EPH-Ephrin signaling	0.006	EPHB3, TIAM1, NGEF, EPHA2, KALRN, EFNB1, RASA1
Focal Adhesion-PI3K-Akt-mTOR-signaling pathway	0.001	DDIT4, EPHA2, LPAR1, PDGFA, PIK3R1, PDGFC, INSR, CDKN1A, JAK2, PHLPP2, VEGFC, VEGFA, IRS2, FGF1, FGF2, FGF7, IL6R, IL4R, HGF, F2R, PGF, CSF1R, FOXO3, FOXO1, FGF14, ITGA10, FGFR2, ITGB4, PIK3CD, SLC2A3, PIK3C2B, ITGB8, NGF, TBC1D1, ITGA5, CREB5, LAMA2, LAMA3, THBS2, ANGPT2, ANGPT1, EGF, LAMB1, PIK3IP1, PPP2R2C, TEK
Focal Adhesion	0.025	MYLK, PDGFA, PIK3R1, PDGFC, JUN, VEGFC, MYLK4, PPP1CB, CCND3, CCND1, HGF, PGF, VCL, CAV3, CAV1, ITGA10, ITGB4, PIK3CD, ITGB8, ITGA5, LAMA2, LAMA3, THBS2, EGF, LAMB1
G alpha (i) signaling events	0.007	LPAR1, FPR1, ADCY4, SAA1, PF4, NPY2R, RGS4, ADORA1, OPN3, HTR1F, CXCL12, GPER, GPSM2, CXCL1, CXCL2, BDKRB2, BDKRB1, SSTR2, RGS18, RGS16, S1PR1, S1PR3, TAS1R1
G alpha (q) signaling events	0.005	GPR68, RGS2, RGS3, F2R, AGTR1, LPAR1, PIK3R1, KALRN, HRH1, GNRH1, ADRA1B, BDKRB2, BDKRB1, EDN1, RGS18, PTGER1, P2RY6, P2RY2, SAA1
Gastrin Signaling Pathway	0.0	CLDN1, CCND1, CDH1, MYC, PRKCE, PRKD1, PIK3R1, FOXO3, FOXO1, SLC9A1, JUN, JAG1, NFKBIA, CDKN1A, JAK2, MMP7, FOS, PPARG, VEGFA
Hair Follicle Development: Induction	0.014	FGF7, MYC, FST, EGF, PTCH1, INHBA, BMP4, FGFR2
JAK/STAT	0.0	IRS2, CCND1, MYC, LEPR, CISH, PIK3R1, FOXO1, JUN, ESR1, JAK2, FOS, IRF1, EGF
Leptin Insulin Overlap	0.026	INSR, IRS2, SOCS1, LEPR, JAK2
Leptin signaling pathway	0.0	IRS2, LEPR, JAK2, CISH, PIK3R1, FOXO1, ESR1
miR-targeted genes in muscle cell - TarBase	0.031	CLDN1, BACH1, ANPEP, CARHSP1, MOV10, NRP1, CDKN1A, PTPRJ, ZEB1, AMIGO2, NT5E, METTL7A, HIPK3, NFIA, NEDD4, FGF2, CCND1, RAB30, PHLDB2, RAI14, NOTCH1, PODXL, SLC38A2, ESR1, CXCL12, ITGB4, CALCOCO2, TNFAIP2, SYNE2, CEBPB, HES1, TXNRD1, SLC4A7, MYO1E, FMNL2
Nuclear Receptors Meta-Pathway	0.0	MYC, PDK4, IL12A, SLC6A13, SDPR, EPHA2, ABCB1, SEC14L1, SLC19A2, JUN, GADD45B, PLK2, SNAI2, CDKN1C, AKAP13, ENC1, IL11, SLC2A14, TSC22D3, B3GNT5, CDC42EP3, AHRR, ANGPTL4, PPARD, HBEGF, AMIGO2, FGD4, SERTAD2, CAP2, GSR, ETNK2, HSPA1A, IRS2, RGS2, CCND1, HGF, FKBP5, FOXO1, GPR115, VDR, ESR1, GCLC, BHLHE40, SPINK13, SLC2A3, PDE4B, ABCC4, ABCC2, GPX3, NRG1, TGFBR3, PRRG4, NRIP1, CCL2, STOM, HES1, UGT1A6, TXNRD1, ALOX5AP
Signaling by Type 1 Insulin-like Growth Factor 1 Receptor (IGF1R)	0.001	IRS2, PIK3R1
TGF-beta Signaling Pathway	0.015	CCND1, MYC, MAP2K3, RUNX2, TP53, ATF3, NEDD4L, PIK3R1, JUN, SMAD3, SMURF2, CAV1, DAB2, CDKN1A, ITGB4, KLF10, FOS, TGFBR3, ZEB1, STAMBPL1, E2F5, CDKN2B
trans-Golgi Network Vesicle Budding	0.02	AP1S3, DNAJC6, SORT1, HIP1R
VEGFA-VEGFR2 Signaling Pathway	0.001	PRKCE, DKK1, TXNIP, PRKD1, LDHA, JUN, JAG1, MOV10, NOX4, SHB, DUSP5, SLC2A14, F3, HBEGF, HSPA1A, NCF2, MAP3K5, MAP2K3, PGF, FOXO4, FOXO3, FOXO1, RCAN1, NUMB, TNFRSF25, CCL2, TRAF3IP2, PNP, EPHA2, PIK3R1, MICAL2, NRP1, PTPRJ, RHOJ, NEXN, AKAP2, VEGFA, FHOD1, CCND1, PLAU, VCL, VCAM1, CAV1, NFKBIA, HSPB1, LDB2, HLX, S1PR1, PTK2B, PDE4DIP, SOD2

List of pathways significantly enriched ($p < 0.05$) in cocultured osteoblasts compared to control osteoblasts and related genes.

significant level of complexity that will require further studies to be elucidated.

In conclusion, our original multi-omics approach, by integrating the adipocyte secretome and the osteoblast transcriptome, provided a number of interactions and signaling pathways paving the way for the understanding of the adipocyte-induced transdifferentiation of osteoblasts. Further biological and functional studies are needed to evaluate the degree to which individual or combined signaling pathways contribute to this phenomenon. Finally, the effectiveness of this integrative strategy for biological data mining could be applied more widely to analyze and decipher the crosstalk between other cell types or tissues.

CRediT authorship contribution statement

Ayyoub Salmi: Data curation, Formal analysis, Methodology,

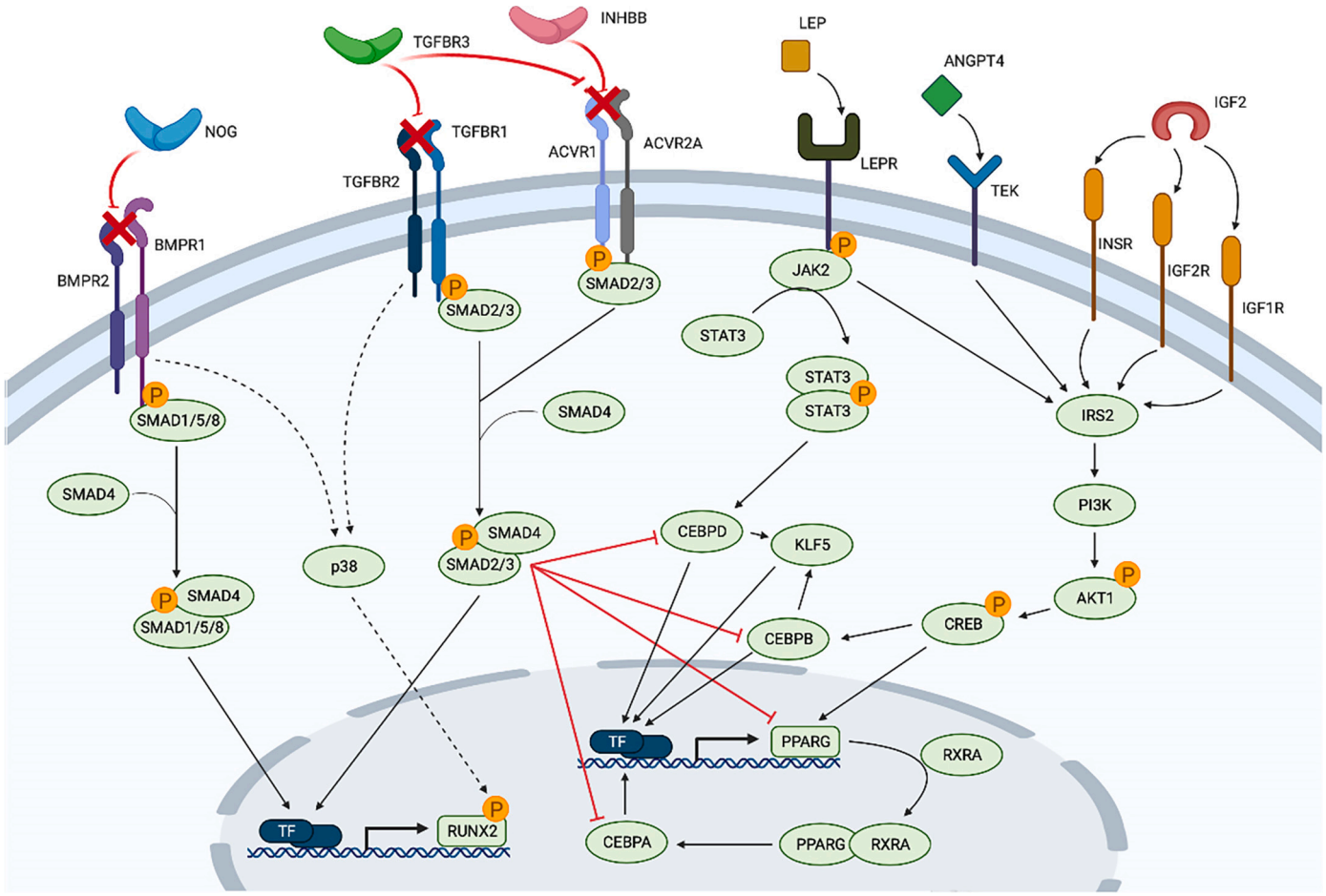

Fig. 6. Proposed pathways implicated in the adipocyte-induced transdifferentiation of osteoblasts. The PI3K-AKT (phosphatidylinositol 3-kinase- protein kinase B) pathway and the JAK2-STAT3 (Janus kinase 2/signal transducers and activators of transcription 3) pathway could promote adipogenesis following the binding of IGF2 (Insulin-like Growth Factor 2), ANGPT4 (Angiopoietin 4) or LEP (Leptin) to their respective receptor. On the other side, the inactivation of the SMAD pathway through the presence in the adipocyte secretome of inhibitors of BMP (Bone Morphogenic Protein), TGFBB (Transforming Growth Factor Beta) and Activin signaling could repress osteogenesis.

Software, Writing – original draft, Writing – review & editing. **Federica Quacquarelli:** Investigation, Methodology, Validation, Writing – review & editing. **Christophe Chauveau:** Funding acquisition, Writing – review & editing. **Aline Clabaut:** Conceptualization, Investigation, Methodology, Validation, Writing – review & editing. **Odile Broux:** Conceptualization, Investigation, Methodology, Supervision, Validation, Writing – original draft, Writing – review & editing.

Declaration of Competing Interest

The authors declare no conflict of interest.

Acknowledgment

The authors thank Olivier Sand from Bilille, Lille for helpful discussions. This work was supported by ULCO. FQ was supported by a fellowship from UFI (Université Franco Italienne).

Appendix A. Supplementary data

Supplementary data to this article can be found online at https://doi.org/10.1016/j.ygeno.2022.110422.

References

[1] S.C. Manolagas, Birth and death of bone cells: basic regulatory mechanisms and implications for the pathogenesis and treatment of osteoporosis, Endocr. Rev. 21 (2000) 115–137, https://doi.org/10.1210/edrv.21.2.0395.
[2] P. Hardouin, V. Pansini, B. Cortet, Bone marrow fat, Joint Bone Spine 81 (2014) 313–319, https://doi.org/10.1016/j.jbspin.2014.02.013.
[3] J. Justesen, K. Stenderup, E.N. Ebbesen, L. Mosekilde, T. Steiniche, M. Kassem, Adipocyte tissue volume in bone marrow is increased with aging and in patients with osteoporosis, Biogerontology 2 (2001) 165–171, https://doi.org/10.1023/A:1011513223894.
[4] P. Meunier, J. Aaron, C. Edouard, G. Vignon, Osteoporosis and the replacement of cell populations of the marrow by adipose tissue. A quantitative study of 84 iliac bone biopsies, Clin. Orthop. Relat. Res. 80 (1971) 147–154.
[5] Q. Chen, P. Shou, C. Zheng, M. Jiang, G. Cao, Q. Yang, J. Cao, N. Xie, T. Velletri, X. Zhang, C. Xu, L. Zhang, H. Yang, J. Hou, Y. Wang, Y. Shi, Fate decision of mesenchymal stem cells: adipocytes or osteoblasts? Cell Death Differ. 23 (2016) 1128–1139, https://doi.org/10.1038/cdd.2015.168.
[6] A. Clabaut, S. Delplace, C. Chauveau, P. Hardouin, O. Broux, Human osteoblasts derived from mesenchymal stem cells express adipogenic markers upon coculture with bone marrow adipocytes, Differentiation. 80 (2010) 40–45, https://doi.org/10.1016/j.diff.2010.04.004.
[7] A. Clabaut, C. Grare, G. Rolland-Valognes, J.-G. Letarouilly, C. Bourrier, T. L. Andersen, T. Sikjær, L. Rejnmark, C. Ejersted, P. Pastoureau, P. Hardouin, M. Sabatini, O. Broux, Adipocyte-induced transdifferentiation of osteoblasts and its potential role in age-related bone loss, PLoS One 16 (2021), e0245014, https://doi.org/10.1371/journal.pone.0245014.
[8] A. Clabaut, C. Grare, T. Léger, P. Hardouin, O. Broux, Variations of secretome profiles according to conditioned medium preparation: the example of human mesenchymal stem cell-derived adipocytes: proteomics and 2DE, Electrophoresis 36 (2015) 2587–2593, https://doi.org/10.1002/elps.201500086.

[9] M.E. Ritchie, B. Phipson, D. Wu, Y. Hu, C.W. Law, W. Shi, G.K. Smyth, Limma powers differential expression analyses for RNA-sequencing and microarray studies, Nucleic Acids Res. 43 (2015) e47, https://doi.org/10.1093/nar/gkv007.
[10] D. Bausch-Fluck, U. Goldmann, S. Müller, M. van Oostrum, M. Müller, O. T. Schubert, B. Wollscheid, The in silico human surfaceome, Proc. Natl. Acad. Sci. U. S. A. 115 (2018) E10988–E10997, https://doi.org/10.1073/pnas.1808790115.
[11] D. Szklarczyk, A.L. Gable, D. Lyon, A. Junge, S. Wyder, J. Huerta-Cepas, M. Simonovic, N.T. Doncheva, J.H. Morris, P. Bork, L.J. Jensen, C. von Mering, STRING v11: protein–protein association networks with increased coverage, supporting functional discovery in genome-wide experimental datasets, Nucleic Acids Res. 47 (2019) D607–D613, https://doi.org/10.1093/nar/gky1131.
[12] A. Subramanian, P. Tamayo, V.K. Mootha, S. Mukherjee, B.L. Ebert, M.A. Gillette, A. Paulovich, S.L. Pomeroy, T.R. Golub, E.S. Lander, J.P. Mesirov, Gene set enrichment analysis: a knowledge-based approach for interpreting genome-wide expression profiles, Proc. Natl. Acad. Sci. 102 (2005) 15545–15550, https://doi.org/10.1073/pnas.0506580102.
[13] D.N. Slenter, M. Kutmon, K. Hanspers, A. Riutta, J. Windsor, N. Nunes, J. Mélius, E. Cirillo, S.L. Coort, D. Digles, F. Ehrhart, P. Giesbertz, M. Kalafati, M. Martens, R. Miller, K. Nishida, L. Rieswijk, A. Waagmeester, L.M.T. Eijssen, C.T. Evelo, A. R. Pico, E.L. Willighagen, WikiPathways: a multifaceted pathway database bridging metabolomics to other omics research, Nucleic Acids Res. 46 (2018) D661–D667, https://doi.org/10.1093/nar/gkx1064.
[14] M. Owen, Marrow stromal stem cells, J. Cell Sci. 10 (1998) 63–76.
[15] J.M. Gimble, C.E. Robinson, X. Wu, K.A. Kelly, The function of adipocytes in the bone marrow stroma: an update, Bone. 19 (1996) 421–428, https://doi.org/10.1016/S8756-3282(96)00258-X.
[16] J. Beresford, J. Bennett, C. Devlin, P. Leboy, M. Owen, Evidence for an inverse relationship between the differentiation of adipocytic and osteogenic cells in rat marrow stromal cell cultures, J. Cell Sci. 102 (1992) 341–351.
[17] M.F. Pittenger, A.M. Mackay, S.C. Beck, R.K. Jaiswal, R. Douglas, J.D. Mosca, M. A. Moorman, D.W. Simonetti, S. Craig, D.R. Marshak, Multilineage potential of adult human mesenchymal stem cells, Science 284 (1999) 143–147, https://doi.org/10.1126/science.284.5411.143.
[18] K. Ecklund, S. Vajapeyam, H.A. Feldman, C.D. Buzney, R.V. Mulkern, P. K. Kleinman, C.J. Rosen, C.M. Gordon, Bone marrow changes in adolescent girls with anorexia nervosa, J. Bone Miner. Res. 25 (2010) 298–304, https://doi.org/10.1359/jbmr.090805.
[19] G. Duque, Bone and fat connection in aging bone, Curr. Opin. Rheumatol. 20 (2008) 429–434, https://doi.org/10.1097/BOR.0b013e3283025e9c.
[20] J.M. Gimble, S. Zvonic, Z.E. Floyd, M. Kassem, M.E. Nuttall, Playing with bone and fat, J. Cell. Biochem. 98 (2006) 251–266, https://doi.org/10.1002/jcb.20777.
[21] S. Muruganandan, R. Govindarajan, C.J. Sinal, Bone marrow adipose tissue and skeletal health, Curr. Osteoporos. Rep. 16 (2018) 434–442, https://doi.org/10.1007/s11914-018-0451-y.
[22] C. Manzoni, D.A. Kia, J. Vandrovcova, J. Hardy, N.W. Wood, P.A. Lewis, R. Ferrari, Genome, transcriptome and proteome: the rise of omics data and their integration in biomedical sciences, Brief. Bioinform. 19 (2018) 286–302, https://doi.org/10.1093/bib/bbw114.
[23] F. Chalmel, E. Com, R. Lavigne, N. Hernio, A.-P. Teixeira-Gomes, J.-L. Dacheux, C. Pineau, An integrative omics strategy to assess the germ cell Secretome and to decipher Sertoli-germ cell crosstalk in the mammalian testis, PLoS One 9 (2014), e104418, https://doi.org/10.1371/journal.pone.0104418.
[24] M. Bonnet, N. Kaspric, K. Vonnahme, D. Viala, C. Chambon, B. Picard, Prediction of the Secretome and the Surfaceome: a strategy to decipher the crosstalk between adipose tissue and muscle during fetal growth, IJMS. 21 (2020) 4375, https://doi.org/10.3390/ijms21124375.
[25] A.R. Guntur, C.J. Rosen, The skeleton: a multi-functional complex organ. New insights into osteoblasts and their role in bone formation: the central role of PI3Kinase, J. Endocrinol. 211 (2011) 123–130, https://doi.org/10.1530/JOE-11-0175.
[26] J. Chen, R. Crawford, C. Chen, Y. Xiao, The key regulatory roles of the PI3K/Akt signaling pathway in the functionalities of mesenchymal stem cells and applications in tissue regeneration, Tissue Eng. B Rev. 19 (2013) 516–528, https://doi.org/10.1089/ten.teb.2012.0672.
[27] W. Yu, Z. Chen, J. Zhang, L. Zhang, H. Ke, L. Huang, Y. Peng, X. Zhang, S. Li, B. T. Lahn, A.P. Xiang, Critical role of phosphoinositide 3-kinase cascade in adipogenesis of human mesenchymal stem cells, Mol. Cell. Biochem. 310 (2008) 11–18, https://doi.org/10.1007/s11010-007-9661-9.
[28] A.W. James, Review of signaling pathways governing MSC osteogenic and Adipogenic differentiation, Scientifica. 2013 (2013) 1–17, https://doi.org/10.1155/2013/684736.
[29] T. Thomas, F. Gori, S. Khosla, M.D. Jensen, B. Burguera, B.L. Riggs, Leptin acts on human marrow stromal cells to enhance differentiation to osteoblasts and to inhibit differentiation to adipocytes, Endocrinology. 140 (1999) 1630–1638, https://doi.org/10.1210/endo.140.4.6637.
[30] J.E. Reseland, U. Syversen, I. Bakke, G. Qvigstad, L.G. Eide, Ø. Hjertner, J. O. Gordeladze, C.A. Drevon, Leptin is expressed in and secreted from primary cultures of human osteoblasts and promotes bone mineralization, J. Bone Miner. Res. 16 (2001) 1426–1433, https://doi.org/10.1359/jbmr.2001.16.8.1426.
[31] E.L. Scheller, J. Song, M.I. Dishowitz, F.N. Soki, K.D. Hankenson, P.H. Krebsbach, Leptin functions peripherally to regulate differentiation of mesenchymal progenitor cells, Stem Cells 28 (2010) 1071–1080, https://doi.org/10.1002/stem.432.
[32] R. Yue, B.O. Zhou, I.S. Shimada, Z. Zhao, S.J. Morrison, Leptin receptor promotes Adipogenesis and reduces osteogenesis by regulating mesenchymal stromal cells in adult bone marrow, Cell Stem Cell 18 (2016) 782–796, https://doi.org/10.1016/j.stem.2016.02.015.
[33] K.J. Motyl, C.J. Rosen, Understanding leptin-dependent regulation of skeletal homeostasis, Biochimie 94 (2012) 2089–2096, https://doi.org/10.1016/j.biochi.2012.04.015.
[34] J.F. Santibanez, J. Kocic, Transforming growth factor-β superfamily, implications in development and differentiation of stem cells, Biomol. Concepts 3 (2012) 429–445, https://doi.org/10.1515/bmc-2012-0015.
[35] M. Morikawa, R. Derynck, K. Miyazono, TGF-β and the TGF-β family: context-dependent roles in cell and tissue physiology, Cold Spring Harb. Perspect. Biol. 8 (2016), a021873, https://doi.org/10.1101/cshperspect.a021873.
[36] B.M. Abdallah, Marrow adipocytes inhibit the differentiation of mesenchymal stem cells into osteoblasts via suppressing BMP-signaling, J. Biomed. Sci. 24 (2017) 11, https://doi.org/10.1186/s12929-017-0321-4.